

# Texture of the uppermost inner core from forward- and back-scattered seismic waves

Vernon F. Cormier \*

*Physics Department, University of Connecticut, 2152 Hillside Road, Storrs, CT 06269-3046, United States*

Received 2 February 2007; received in revised form 31 March 2007; accepted 1 April 2007

Available online 11 April 2007

Editor: R.D. van der Hilst

## Abstract

Body waves interacting with the boundary of the solid inner core at narrow and wide angles of incidence provide independent constraints on a heterogeneous texture that may originate from the process of solidification. The equatorial, quasi-eastern hemisphere, of the uppermost 50–100 km of the inner core is characterized by a higher isotropic P wave velocity, lower  $Q_\alpha$ 's inferred from PKiKP, and simpler PKiKP pulses compared to adjacent regions in the western hemisphere and polar latitudes. Compared to this region, the adjacent western (primarily Pacific) equatorial region is characterized by higher  $Q_\alpha$ 's and a higher level of coda excitation following PKiKP. Lateral variations in both inner core  $Q_\alpha$  inferred from transmitted PKiKP and inner core heterogeneity inferred from the coda of reflected PKiKP can be modeled by lateral variations in a solidification fabric. In an actively crystallizing eastern equatorial region, characterized by upwelling flow in the outer core, fabrics that explain strong attenuation and the absence of attenuation and velocity anisotropy in short range ( $120^\circ$ – $140^\circ$ ) PKiKP and weak PKiKP codas have an anisotropy of scale lengths with longer scale lengths in the vertical direction, perpendicular to the inner core boundary. In less actively solidifying regions in the equatorial western hemisphere, longer scale lengths tend to be more parallel to the inner core boundary, consistent with outer core flow tangent to the inner core boundary or viscous shearing and recrystallization in the horizontal direction away from more actively crystallizing regions in the eastern hemisphere. This texture is less effective in attenuating PKiKP by forward scattering. Lateral variation in the equatorial western hemisphere between vertical versus horizontal oriented plate-like textures may explain lateral variations from weak to strongly back-scattered PKiKP coda and from strong to weak velocity and attenuation anisotropy in short range PKiKP.

© 2007 Elsevier B.V. All rights reserved.

*Keywords:* inner core; outer core; scattering; attenuation; anisotropy; synthetic seismograms; geodynamo

## 1. Introduction

Seismic wavefields interacting with the uppermost 300 km of the inner core, although limited in uniformity of geographic sampling, reveal this region to have strong lateral variations in elastic structure, anisotropy,

attenuation, and scattering. Forward scattering by a complex fabric or texture in the uppermost inner core has been shown to be a viable alternative to viscoelasticity to explain high elastic attenuation in this region [1,2]. Vidale and Earle [3] confirmed the existence of a scattering fabric in this region from the back-scattered coda of high-frequency PKiKP waves. A recent global study of back-scattered PKiKP coda by Leyton and Koper [4] concludes that coda shapes of PKiKP are best

\* Tel.: +1 860 486 3547; fax: +1 860 486 3346.

E-mail address: [vernon.cormier@uconn.edu](mailto:vernon.cormier@uconn.edu).

explained by volumetric scattering in the uppermost inner core and that scattering may be a significant contribution to the attenuation inferred from the pulse broadening and amplitude reduction of PKiKP waveforms. The spatial distribution of the 1–10 km scale lengths of heterogeneity responsible for the observed scattering may also be important in explaining lateral variations in elastic anisotropy for wavelengths long with respect to the heterogeneity scales. The complexity of these lateral variations in texture may be responsible for continuing difficulties in seeking a simple global model of inner core anisotropy.

The detailed texture of uppermost inner core is important for understanding how the inner core is solidifying from the liquid outer core, possibly providing a mechanism for compositional convection that can drive the geodynamo [5,6]. The origin of lateral variations in the uppermost inner core may be related to lateral differences in solidification or viscous flow and recrystallization, which are closely coupled to variations in fluid flow at the bottom of the liquid outer core. Laboratory experiments examining the complex textures of crystallized ices and hcp metals in convecting and rotating melts have led Bergman et al. [7–9] to speculate that “the convective pattern at the base of the outer core is recorded in the texture of the inner core”. If true, lateral variations in outer core flow would be preserved in lateral variations in texture of the inner core.

Studies of scattering in the inner core have thus far only considered the effects of isotropically distributed scale lengths of heterogeneity. Since the crystallization and flow induced textures observed by Bergman et al. [7–9] are characterized by a strong anisotropy in scale lengths, it is of interest to consider the effects of elastic scattering in random media having a geometric anisotropy of scale lengths. A recent study of this type of media by Hong and Wu [10] predicts a large change in the relative behavior of forward- versus backward-scattering for waves incident parallel to, versus perpendicular to, the direction in which longer scale lengths are oriented. For application to the inner core, the relevant wave types to examine for evidence of this change are the coda of PKiKP, for back-scattering effects, and the pulse broadening and amplitude reduction of PKiKP, for forward-scattering effects (Fig. 1).

## 2. Texture effects on PKiKP and PKIKP

### 2.1. Summary results

Fig. 2 summarizes the waveform effects expected for forward and back scattering from anisotropic textures

predicted from the results obtained by Hong and Wu from numerical modeling in the crust and upper mantle. The back-scattered PKiKP coda are a quantitative prediction of the effects of the exact inner core fabrics shown. The pulse broadening and attenuation of PKiKP due to forward scattering are qualitatively estimated by assuming 1-D profiles along the PKiKP paths and comparing with previous calculations for transmitted waveforms [1,2]. Details of the modeling, including effects of isotropic heterogeneity distributions, are discussed in Section 2.2 for the back-scattered coda of reflected PKiKP and Section 2.3 for the forward-scattering effects on transmitted PKiKP.

The fabric stretched vertically in Fig. 2, perpendicular to the inner core boundary, might represent that produced by columnar crystals growing radially outward from a newly solidified inner core. The fabric stretched horizontally in Fig. 2, parallel to the inner core boundary, might represent that produced by older fabric created by flow and recrystallization, moving material from an actively crystallizing region laterally to another region by the mechanism of isostatic relaxation proposed by Yoshida et al. [11]. In this mechanism, material flows horizontally from a more actively crystallizing region to a slower crystallizing region to maintain isostatic equilibrium and inner core sphericity. P waves transmitted through the vertically oriented fabric are attenuated and have broadened pulses. Pulse broadening partly occurs because high frequency energy is stripped out of the pulse by back scattering of higher frequency energy. Time delays

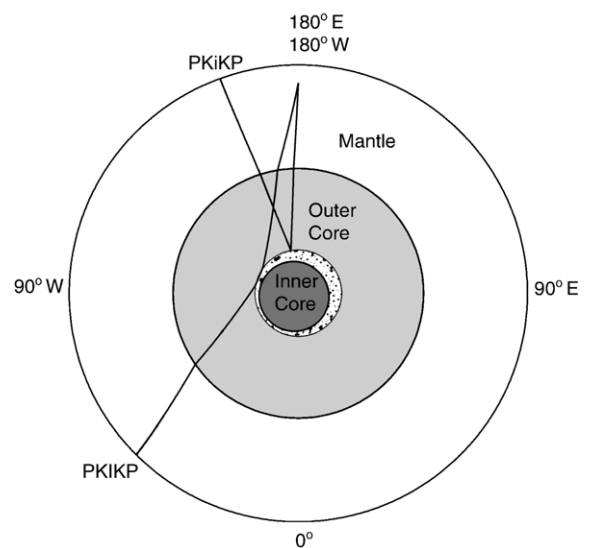


Fig. 1. Ray paths of PKiKP and short range PKIKP. Large-scale lateral variation in an elastically isotropic uppermost inner core is shown in a polar cross section.

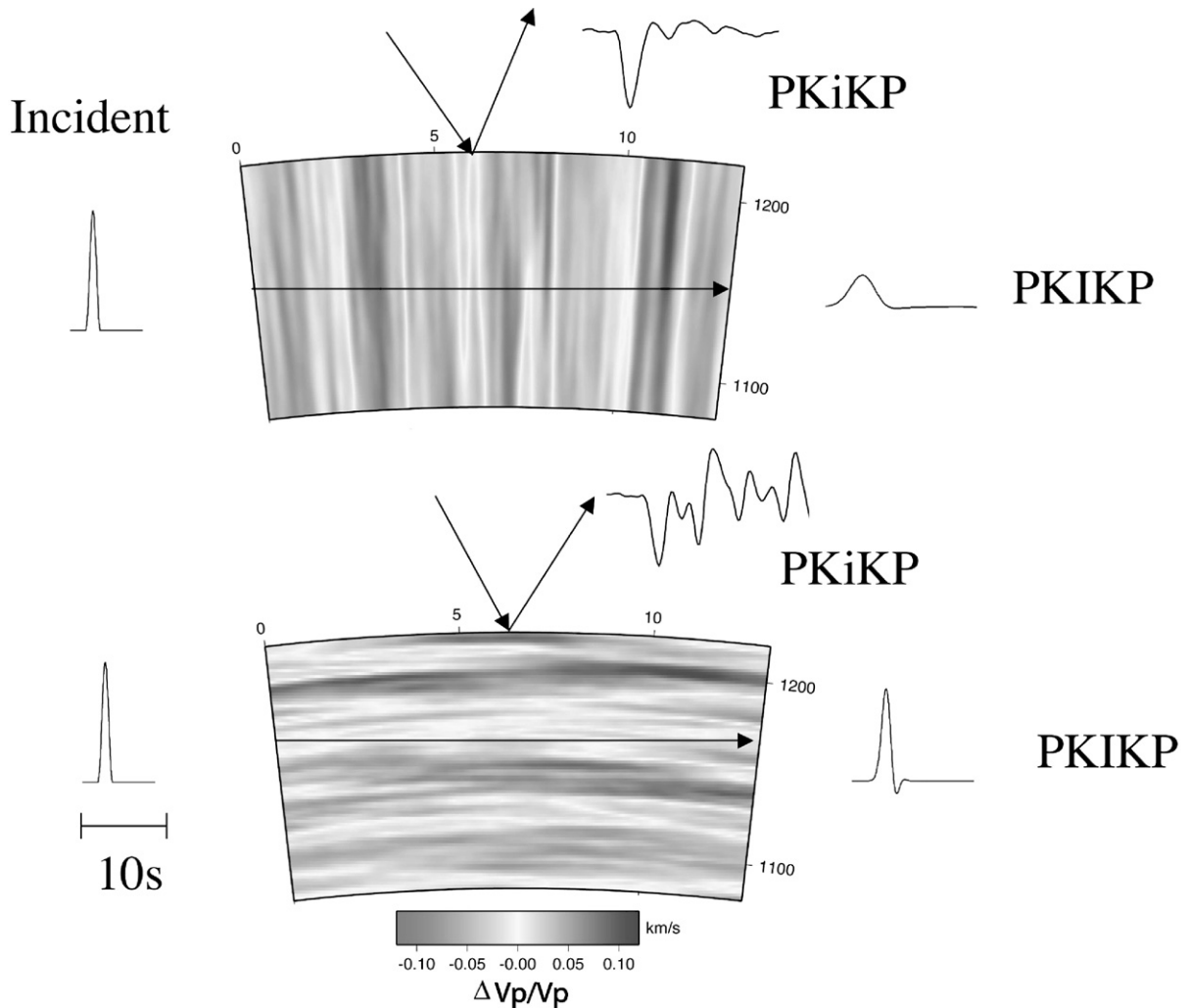


Fig. 2. Waveform effects compared for vertical (top) and horizontal (bottom) oriented fabric in the uppermost inner core on transmitted PKiKP at  $120^{\circ}$ – $140^{\circ}$  range and reflected PKiKP at  $0^{\circ}$  to  $50^{\circ}$  range.

of energy scattered in the forward direction also act to broaden the pulse. Transmission through fabric oriented parallel to the direction of transmission results in much less attenuation and pulse broadening because many fewer regions of strong impedance gradient are encountered within the Fresnel volume of sensitivity of the transmitted PKiKP wave. Strong back scattering can be observed in the coda of PKiKP waves reflected from the horizontally oriented fabric but not from the fabric oriented vertically.

In summary, PKiKP pulse broadening and attenuation is anti-correlated with the coda excitation of PKiKP in any fabric in which heterogeneity scale lengths differ significantly in horizontal and vertical directions. In contrast, the effects of isotropic heterogeneity will tend to make PKiKP pulse broadening and attenuation po-

sitively correlate with the coda excitation of PKiKP. The following sub-section details the modeling of effects of both isotropic and anisotropic heterogeneity.

## 2.2. Modeling of reflected PKiKP and back-scattered coda

Back-scattered PKiKP coda are modeled using the 2-D pseudospectral code and techniques described by Cormier [12], which are closely related to those described by Kennett and Furumura [13]. This fully numerical approach to modeling insures that all effects of multiple back and forward scattering are included. Time and spatial sampling are taken to be appropriate for synthesizing PKiKP waves in a 2-D cylindrical model for frequencies up to 1 Hz at ranges up to  $90^{\circ}$ .

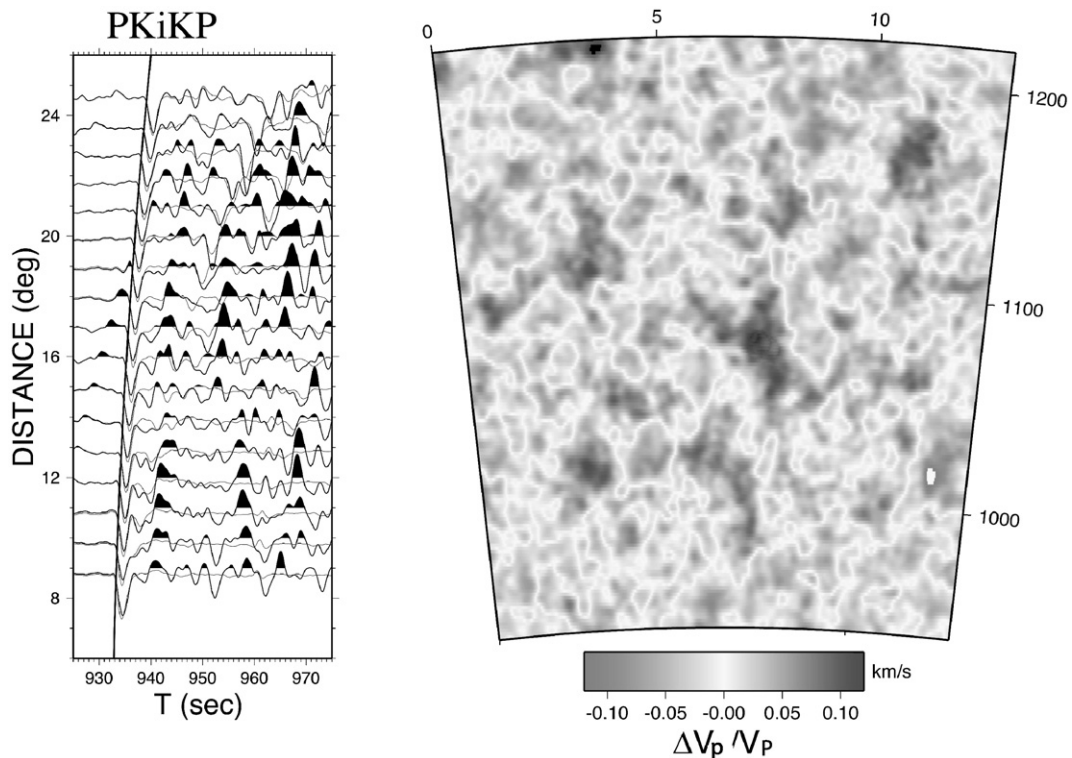


Fig. 3. Synthetic displacement record section (left) of PKiKP reflected by an inner core texture having an isotropic distribution of heterogeneity scale lengths (right). Synthetic displacement record section for a homogeneous reference earth model (PREM) are the lighter traces.

Stability and minimal grid dispersion at this range required a choice of  $\Delta\theta=0.007627$  radians ( $6371 * \Delta\theta = \Delta x=4.85$  km at Earth's surface),  $\Delta z=3$  km,  $\Delta t=0.025$  s, a  $2048 \times 2048$  grid size, and 40,000 time steps. The model is decomposed and calculations are parallelized across 8 dual 2 GHz processors. Each P-SV run for a vertical point force, integrating equations of motion in a velocity–stress formulation, required about 40 h processing time. A line to point source correction is applied, ground velocity converted to ground displacement, and the result low pass filtered with a two pole Butterworth filter having a corner at 0.8 Hz. Figs. 3–5 show the results of modeling the back-scattered coda of PKiKP for three types of inner core fabric. Although the complete wavefield is synthesized for receivers at ranges up to  $90^\circ$ , only in the  $0^\circ$  to  $30^\circ$  range is PKiKP large enough in amplitude and well separated from larger amplitude phases to easily compare the coda excitation relative to the main pulse. Leyton and Koper's [4] observations were restricted to ranges greater than  $30^\circ$ , where the inner core reflection coefficient is smallest and where any PKiKP observation will emphasize the effects of inner core scattering. In this distance range, recording at dense small aperture arrays and beamforming is necessary to isolate PKiKP in the midst of

much larger amplitude phases arriving from different angles at nearby arrival times. At shorter ranges (less than  $30^\circ$ ) PKiKP is well separated from other phases and has larger amplitude, making it easier to identify and display in synthetic profiles at single receivers without beamforming. Differences between the excitation of PKiKP coda between  $10^\circ$  to  $30^\circ$  and the excitation of PKiKP coda observed at the slightly longer range studied by Leyton and Koper [4] are likely to be small. In each example (Figs. 3–5), synthetic seismograms for the heterogeneous model are overlaid on those for a PREM [14] homogeneous inner core model. The PREM synthetics for ground displacement have a simple symmetric pulse, nearly identical in shape to an input Gaussian source–time function, followed by a nearly flat coda, demonstrating the stability and numerical accuracy of the calculation.

Models of heterogeneous fabrics in the inner core are created using the techniques described by Frankel and Clayton [15]. An exponential autocorrelation is assumed that has a flat spatial spectrum with a corner that decays for wavenumbers corresponding to wavelengths less than 20 km. The RMS perturbation in P velocity is 10%. Perturbations in S velocity are assumed to be double those in P velocity. Since realistic density perturbations

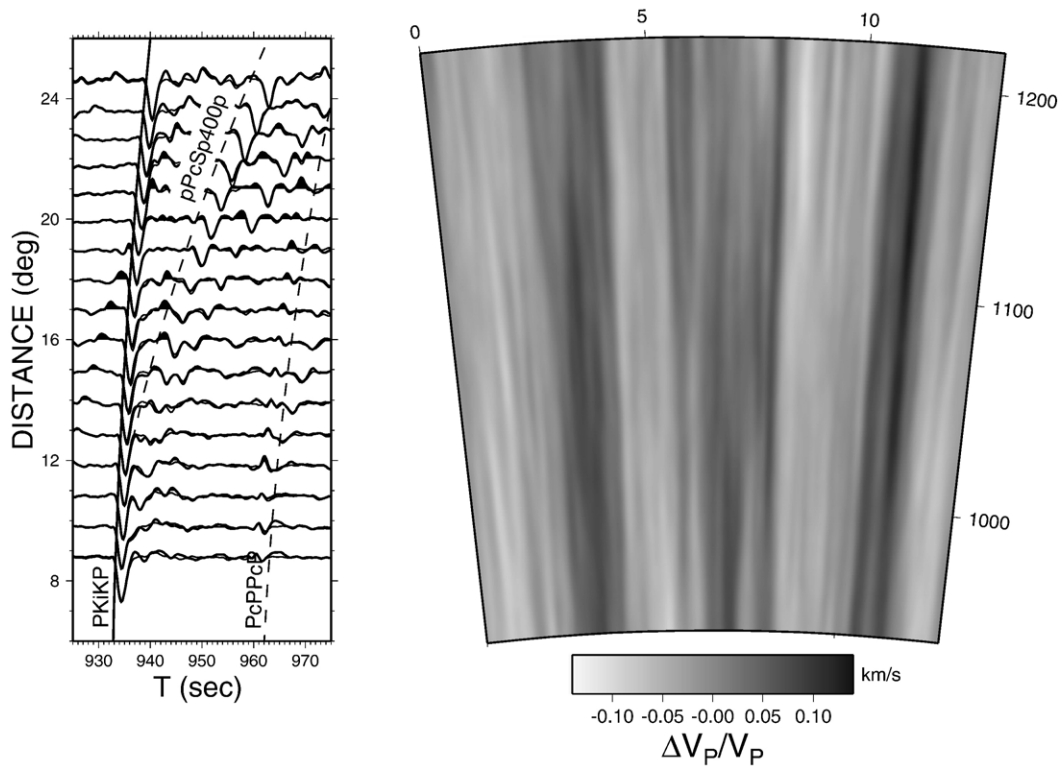


Fig. 4. Synthetic displacement record section (left) of PKiKP reflected by an inner core texture having an anisotropic distribution of heterogeneity scale lengths (right) with longer scale lengths in the vertical direction. Synthetic displacement record section for a homogeneous reference earth model (PREM) are the lighter traces. Arrival times of additional coherent weak phases are shown by dashed lines, where the phase nomenclature of Ward [16] is adopted for pPcSp400p.

are likely to be an order of magnitude smaller than those for velocity, no density perturbations are assumed.

Fig. 3 shows the effects of a fabric having an isotropic distribution of scale lengths, independent of direction with respect to the inner core boundary. Note that with 10% P velocity fluctuations, this fabric can create a strong coda, but the individual wiggles of the coda in this range are weaker than the main pulse. A vertically oriented fabric with an anisotropic distribution of scale lengths (Fig. 4) produces a very weak scattered coda in PKiKP. The coda level is nearly indistinguishable from that in a background PREM. What coda exists is primarily due to reflections and conversions at radially symmetric boundaries in the model, evident in the coherent moveouts identified as pPcSp400p and PcPPcP identified in Fig. 4. Horizontally oriented fabric (Fig. 5) generates very strong coda in PKiKP with individual coda pulses equal or stronger than the direct pulse. Hence a strong back-scattered PKiKP coda can be generated by either isotropically distributed heterogeneity in the inner core at high levels (10%) of perturbation or by anisotropically distributed heteroge-

neity at lower levels (5 to 7%) of perturbation with longer scale lengths parallel to the inner core boundary. Small or absent PKiKP coda can be consistent either with a homogeneous inner core or by anisotropically distributed heterogeneity with longer scale lengths perpendicular to the inner core boundary.

### 2.3. Modeling of forward-scattering effects on transmitted PKiKP

Previous studies have explored the effects of 1-D and 3-D inner core isotropic heterogeneity on transmitted PKiKP amplitudes and pulse broadening. For 1-D heterogeneity, corresponding to PKiKP propagating perpendicular to the long axis of anisotropically distributed heterogeneity, forward-scattering effects can be calculated from the transmitted wavefield by a reflectivity approach assuming normal incidence on a randomly fluctuating plane-layered medium. RMS P velocity fluctuations on the order of 10% in the direction of the transmitted wave for scale lengths on the order of the shortest lengths scales in Figs. 3–5 correspond to an

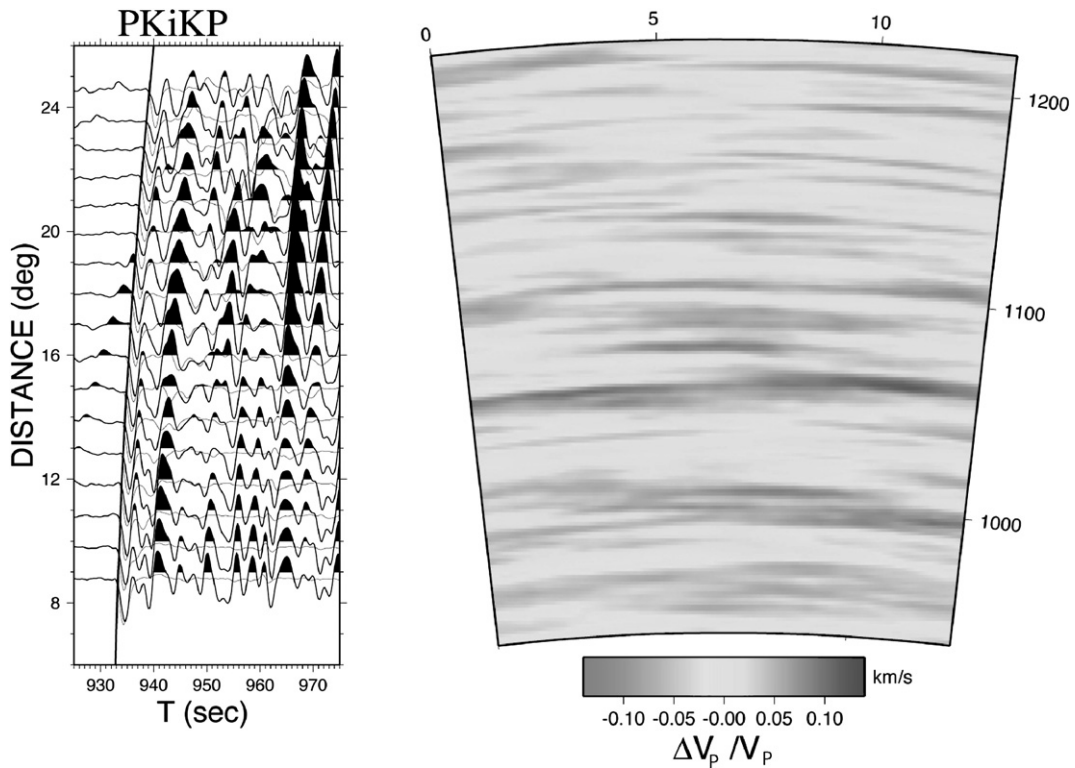


Fig. 5. Synthetic displacement record section (left) of PKiKP reflected by an inner core texture having an anisotropic distribution of heterogeneity scale lengths (right) with longer scale lengths in the horizontal direction. Synthetic displacement record section for a homogeneous reference earth model (PREM) are the lighter traces.

apparent  $Q_\alpha$  of 200 inferred from the pulse shapes and amplitudes of PKiKP [1]. Similar length scales and velocity fluctuations for 3-D isotropically distributed heterogeneity, using an approximate theory for forward scattering (DYCEM by Kaelin and Johnson [17]), correspond to  $Q_\alpha$ 's on the order of 100 to 300 [2].

### 3. Links between lateral variations in inner core structure and texture

#### 3.1. Constraints and observations

Due to sparse distributions of sources and receivers in polar regions, the inner core is most densely sampled by PKiKP waves having more equatorially oriented paths. For this reason, discussion in this section will be primarily confined to equatorial variations. Fig. 6 summarizes three types of lateral variations of structure in the uppermost inner core, each differing in sensitivity in different ways to texture. Fig. 6a shows thickness contours of a lower velocity region in the uppermost inner core inferred from seismic waveforms in a study by Stroujkova and Cormier [18]. That study inferred a rapid transition in depth to higher velocities, which

generates a triplication or multipathing in the  $130^\circ$  to  $140^\circ$  range of PKiKP+PKiKP waveforms. The thickest transition layer (40 km) was found in the equatorial region of the eastern hemisphere. Song and Helmberger [19] suggest that a thicker (95 km) transition layer exists near western edge of this anomaly, but note that models reproducing observed waveform perturbations are non-unique with multiple sharp transitions possible in the upper 100 to 200 km of the inner core with significant lateral variations.

Fig. 6b summarizes the results obtained by Leyton and Koper [4] for the excitation of PKiKP coda by scattering in the upper 300 km of the inner core. The most intense region of scattered coda following PKiKP occurs in the equatorial eastern hemisphere just east of the transition layer contoured in Fig. 6a. Part of their analysis finds weaker scattering in the easternmost region of the closed contour of the thickest transition layer in Fig. 6a. In array observations at shorter ranges ( $10^\circ$  to  $30^\circ$ ) than those analyzed by Leyton and Koper, no evidence exists of any significant inner core scattering from the coda of PKiKP reflected from the inner core in the middle of the 40 km thick closed contour of the transition layer in

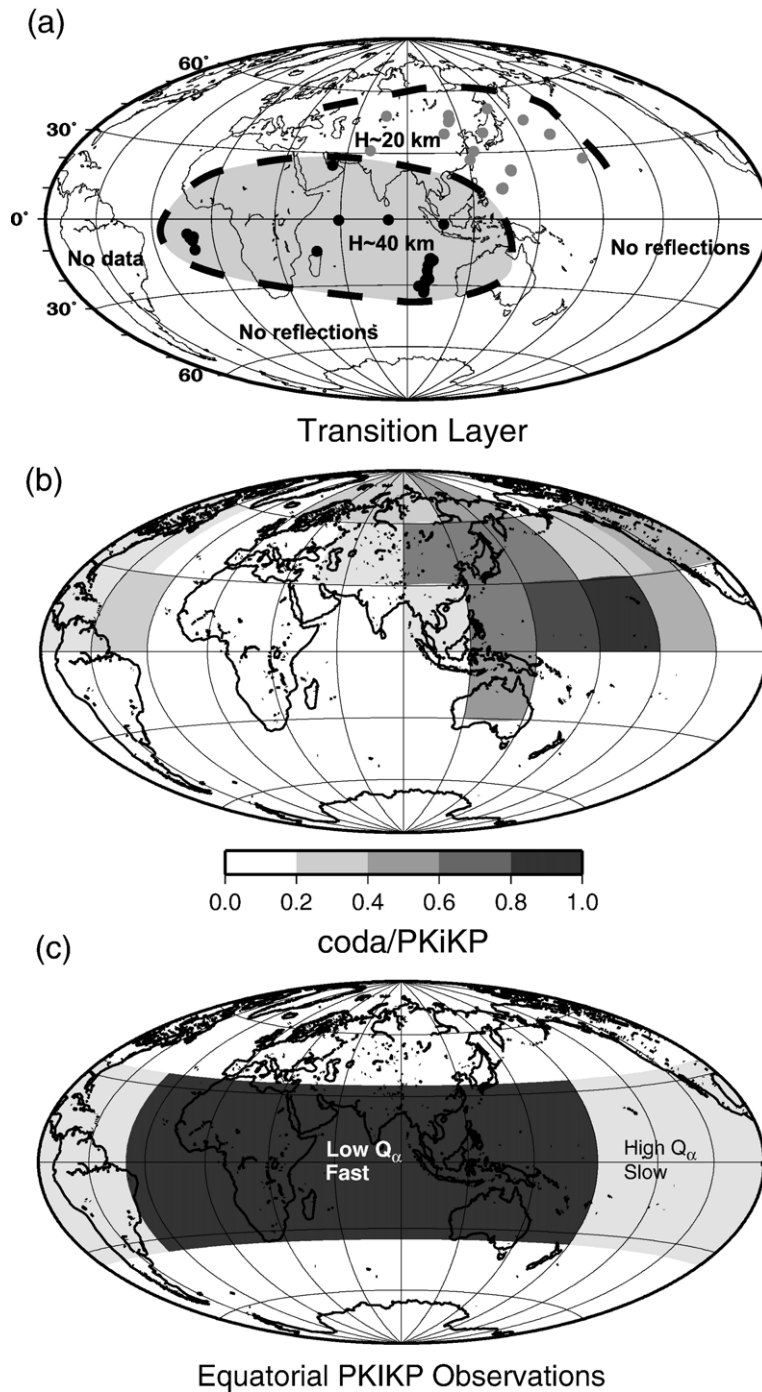


Fig. 6. (a) Contours thickness of anomalous lower velocity layer in the uppermost inner core determined in the study by Stroujkova and Cormier [18]; (b) excitation of back-scattered PKiKP coda from heterogeneity in the uppermost inner core determined in the study by Leyton and Koper [4]; (c) summary of lateral variations in attenuation and P velocity in the equatorial region of the inner core determined in the study by Yu and Wen [22].

Fig. 6a [20 and Stroujkova, personal communication] nor from PKiKP reflected at points near  $30^\circ$  N,  $140^\circ$  E within the neighboring closed contour of the 20 km thick transition layer [21].

Fig. 6c summarizes the results of studies by Yu and Wen [22] for travel times and attenuation of PKiKP waves transmitted through the uppermost inner core. This study interprets the PKiKP/PKiKP amplitude ratio

in terms of path averaged  $Q$ 's, travel time variations in terms of isotropic and anisotropic variations, and attempts to integrate a multiplicity of studies [23–34]. These studies generally agree that the upper inner core of the eastern equatorial hemisphere ( $40^\circ$  to  $180^\circ$  E) is elastically isotropic and has a strong depth dependence of attenuation, with  $Q_\alpha$  increasing from 300 near its boundary to 600 below 300 km depth. Results of the western hemisphere ( $180^\circ$  W– $40^\circ$  E) of the inner core are much more difficult to generalize. This region is characterized by smaller scale lateral variations. It generally has weaker attenuation (higher  $Q_\alpha$ ). Yu and Wen's [22] average attenuation model for the western hemisphere has  $Q_\alpha=600$ . The western hemisphere exhibits strong lateral variations in velocity and attenuation anisotropy, the upper 80 km of the inner core in the eastern hemisphere beneath Africa being characterized by pronounced attenuation and velocity anisotropy, but with velocity and attenuation anisotropy beneath the Caribbean Sea and Central America becoming strong only after 180 km depth.

### 3.2. Interpretation

The interpretations of  $Q$  effects of texture are simpler than those of anisotropy. This is due to continuing uncertainties in the lattice structure and elasticity of inner core minerals and to problems in unraveling a complex lateral and depth dependent variation in velocity anisotropy in the western hemisphere from a limited sample of paths. Evidence of scattering from the upper 300 km of the earth's inner core suggests that some, if not all, of the attenuation observed in P waves transmitted through this region may be due to scattering. The relative portion of attenuation attributable to scattering versus viscoelasticity, however, is still unknown. Hence, any interpretation of attenuation as an effect of scattering from a heterogeneous fabric must also consider the alternative possibility that either some or most of the attenuation might be due to viscoelasticity.

#### 3.2.1. Eastern hemisphere

Three simple interpretations may exist for the more uniform behavior on PKiKP and PKIKP of the eastern hemisphere of the uppermost inner core: waveform effects are due to either the effects of (1) a homogeneous isotropic structure and viscoelasticity, (2) heterogeneous structure with an isotropic distribution of scale lengths, or (3) forward and back scattering by very specific texture. In interpretation (2) strong heterogeneity with isotropically distributed scale lengths can explain strong PKiKP coda, high PKIKP attenuation and weak shape preferred

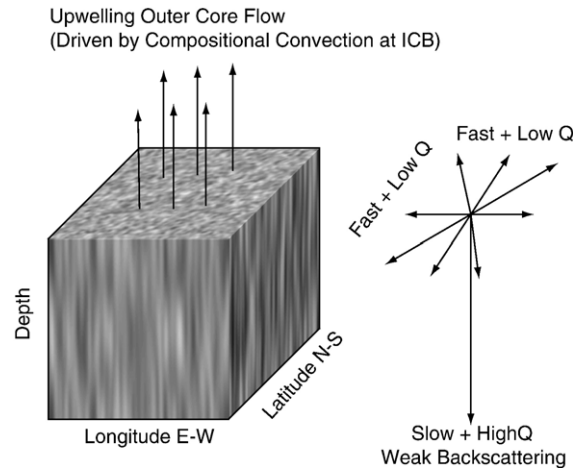


Fig. 7. Possible texture in the equatorial eastern hemisphere to explain isotropic velocities and high isotropic attenuation of transmitted PKIKP ( $120^\circ$  to  $140^\circ$ ) and lack of back-scattered coda of PKiKP.

orientation (SPO) anisotropy. In interpretation (3), the velocity isotropy and high attenuation of PKIKP at grazing incidence to the ICB can be explained by vertical oriented structures having scale lengths long in vertical direction and short scale lengths in the two orthogonal horizontal directions, parallel to the inner core boundary (Fig. 7). Such a structure would exhibit a low  $Q_\alpha$  inferred from forward scattering of short range PKIKP waves transmitted through the uppermost inner core in any direction with respect to the rotation axis. Short range ( $120^\circ$  to  $140^\circ$ ) PKIKP's sampling the uppermost inner core in the equatorial eastern hemisphere are fast relative to those observed in much of the western hemisphere [22–34]. Hence, any intrinsic anisotropy of grains in the uppermost inner core in this region must be such that the elongated vertical axis of the heterogeneity scale lengths lies in at least one of the two slow directions of intrinsically anisotropic grains. The remaining slow and fast directions must be randomly distributed in planes parallel to the inner core boundary, such that the average velocity of short range ( $120^\circ$  to  $140^\circ$ ) PKIKP is relatively faster and isotropic compared to short range PKIKP sampling regions outside the equatorial eastern hemisphere. The rays of the longer range PKIKP's in or near the equatorial plane of the eastern hemisphere cross fewer grain boundaries and are thus less attenuated by forward scattering, perhaps accounting for the strong depth dependence of attenuation seen in the eastern hemisphere, similar to the original fabric interpretation of Bergman [35].

#### 3.2.2. Western hemisphere

Interpretations of effects on PKIKP and PKiKP waves sampling the equatorial western hemisphere are

more complex and always need to invoke the existence of at least some scattering. Assuming that attenuation is primarily by scattering, higher  $Q_\alpha$  for equatorial paths in the western hemisphere can be explained by a tendency for the longer axis of heterogeneity scale lengths to lie parallel to the equatorial plane. More pronounced attenuation and velocity anisotropy in the western hemisphere can be explained by the vertically dipping plate-like fabric shown in Fig. 8, in which polar paths will exhibit stronger attenuation than equatorial paths and in which the slow direction will lie along the east–west stretched direction of heterogeneity for equatorial paths. Lateral variations in PKiKP coda excitation can be explained by either superposing a laterally varying isotropic distribution of heterogeneity scale lengths, or by a transition to the fabric shown in Fig. 9, in which plate-like heterogeneity lies parallel to the inner core boundary. A test for the existence of the fabric illustrated in Fig. 9 would be to check if short range PKiKP exhibits unusually weak attenuation and little velocity and attenuation anisotropy in the equatorial patches that are observed to have strong back-scattered PKiKP coda. Transitions between the textures illustrated in Figs. 8,9 may be at least partially responsible for the lateral gradients in inner core anisotropy beneath Central America observed in polar paths of PKiKP between the South Sandwich Islands and College Alaska [25].

#### 4. Implications for outer core flow, compositional convection, and the geodynamo

From laboratory experiments on solidifying ices and metals, Bergman et al. [7–9] have suggested that solidification textures are correlated with flow directions

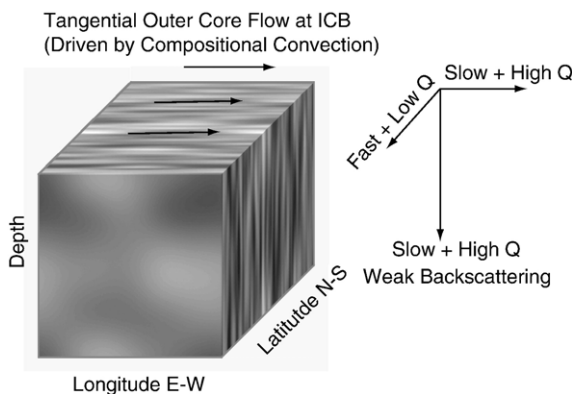


Fig. 8. Possible dominant texture in the equatorial western hemisphere to explain more pronounced equatorial versus polar anisotropy in velocity and attenuation of transmitted PKiKP ( $120^\circ$  to  $140^\circ$ ) and weaker back-scattered coda of PKiKP.

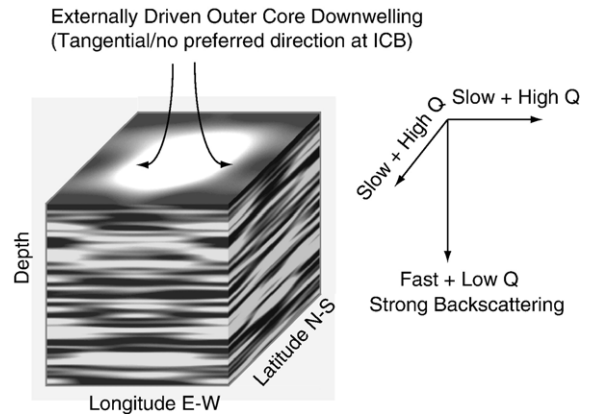


Fig. 9. Possible texture in certain regions of the western hemisphere to explain isotropic velocities, weak isotropic attenuation of transmitted PKiKP ( $120^\circ$  to  $140^\circ$ ), and high amplitudes of back-scattered coda of PKiKP.

in the liquid region at the solid–liquid boundary. An important result of Bergman’s experiments with hcp metals is that vertically oriented plate-like textures develop at the solid–liquid boundary. For convectively driven flow, these platelets are perpendicular to the flow direction, but for externally driven flow these platelets are parallel to the flow direction [8,36]. Figs. 7–9 have assumed that the inner core is an hcp metal and that horizontal flow is convectively driven. If horizontal flow is instead externally driven, the orientation of horizontal flow in Fig. 7 should be rotated  $90^\circ$ . Because some disagreement still exists for ab initio calculations of elastic constants in the fast direction of hcp iron at inner core temperatures and pressures [37,38], Figs. 7–9 simply label the fast axis direction without specifying whether it is the  $c$  axis or one of the basal plane axes.

The texture illustrated in Fig. 8 might be consistent with flow tangent to the inner core boundary dominantly in either the east–west direction (convectively driven flow) or north–south direction (externally driven flow) along most of the equatorial region of the western hemisphere. This region would exhibit attenuation and velocity anisotropy in short range PKiKP, fast velocity correlating with strong attenuation and slow velocity with weak attenuation, and a weak PKiKP coda. In a few regions along the equatorial western hemisphere exhibiting strong PKiKP coda, a texture of the type shown in Fig. 9 might be consistent with a locally strong vertical flow near the inner core boundary. In these regions, PKiKP will have strong coda due to back scattering from plate-like structures parallel to the inner core boundary. Transmitted short range PKiKP through these regions should exhibit low attenuation (high  $Q_\alpha$ ) with little or no velocity and attenuation anisotropy.

In the absence of strong horizontal flow, a texture may develop with predominantly vertical columnar crystals of the type shown in Fig. 7. A texture of this type may be required by the behavior of PKIKP and PKiKP in the equatorial eastern hemisphere. This may be a region of dominant upwelling from the inner core boundary, associated with a relatively lower viscosity fluid enriched in lighter elements. Motion of the lower viscosity fluid in this region of the outer core may be characterized by smaller scale turbulent structures perhaps responsible for stronger magnetic secular variation in the eastern hemisphere. In the western hemisphere, fluid motion near the equator may be dominated by effects of higher fluid velocities in a cylinder tangent to the inner core with vertical plate-like textures oriented parallel to the east–west direction (Fig. 8). Localized regions of equatorial western hemisphere texture may have flat-lying plate-like structures that back scatter energy into the coda of PKiKP (Fig. 9). Such textures are not consistent with those observed at the boundaries of crystallizing solids, but may represent the effects of internal strain induced by either isostatic [11] or Maxwell [39] stresses moving material laterally away from newly crystallized regions. These non-actively crystallizing regions may be correlated with regions of vertical down-flow in the outer core that compensate for vertical up-flow in the eastern equatorial region. The region of strongest possible down-welling correlates with a region of low magnetic secular variation in the Pacific [40], which may be consistent with a more viscous, less turbulent, outer core fluid in this region.

The possible existence of lateral variations in up- and down-welling flow may require lateral variations in at least the density and viscosity in the outer core, if not also its bulk modulus. Lateral variations in the compressional wave velocity at the bottom of the outer core have been proposed in the study by Yu et al. [34], with the eastern hemisphere of the lowermost outer core being more PREM-like and hence stably stratified, and the western hemisphere having a reduced gradient near the inner core boundary (Fig. 10). A recent study by Zou et al. [41] of the compressional waves diffracted around the inner core boundary favors a global model of reduced  $K$  velocity gradient near the inner core boundary and proposes a denser stagnant layer in that region. Since the data in the Zou et al. study are strongly weighted towards paths in the western hemisphere, it is generally consistent with the western hemisphere of the lowermost outer core model of Yu et al. [34]. Lateral variations in the amplitude of the direct pulse of reflected PKiKP point to the existence of a possible transition region of rigidity in or near the inner core

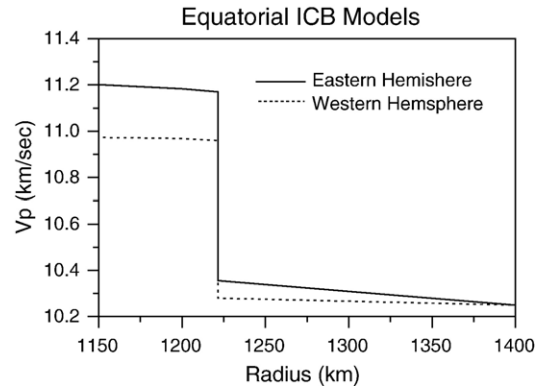


Fig. 10. Summary of eastern and western hemispherical P velocity models of the uppermost inner core and lowermost outer core from and Yu et al. [34].

boundary [42]. Such lateral variations in the outer core density, viscosity, and velocity defy the conventional wisdom of a chemically homogeneous, low viscosity, vigorously convecting, outer core [43]. They may, however, be a natural consequence of the gravitationally driven up- and down-welling motions of compositional convection that stirs the outer core fluid and drives the geodynamo. Recent studies of PcP and PKP travel times by Soldati et al. [44] have reversed an earlier conclusion of Piersanti et al. [45], finding that density heterogeneity in the outer core may equal or exceed 0.1% and that this heterogeneity is positively correlated with topography on the core–mantle boundary.

If the flow structure of the outer core were recorded in the texture of the uppermost inner core, lateral variations in inner core texture would tend to be erased by a constant differential rotation rate of the inner core. This would make it difficult to explain the observed differential rotation unless it is due to either a wobble or precession or to time variations in the structure within or near the uppermost inner core. An additional argument against a constant differential rotation rate may be the correlation between hemispherical variations in inner core structure and structure near the core–mantle boundary (e.g., [46]) especially the correlation between a change in inner core fabric and a strong lateral gradient in CMB topography and P velocities in the lowermost mantle near 180° E/180° W longitude. If the net rate of differential rotation or wobble of the inner core averages to zero over time, then variations in core–mantle boundary structure may be coupled to lateral variations in texture and structure in the uppermost inner core by controlling fluid flow in the outer core, which may be coupled to longitudinal variations in the intensity of magnetic secular variations [47].

## 5. Conclusions

The existence of scattering by a fabric of small-scale heterogeneities in the uppermost inner core has been confirmed. The inferred scale lengths and intensities of fluctuation are in a domain that is capable of producing attenuation in body waves transmitted through the inner core. Intrinsic viscoelasticity will also contribute to the total attenuation inferred from PKiKP waveforms, but the ratio of viscoelastic attenuation to scattering attenuation is still unknown. Until this ratio is accurately estimated, it is difficult to make quantitative predictions about the effects the heterogeneous texture of the uppermost inner core, but several new qualitative predictions are possible.

Laboratory experiments on solidifying textures of hcp metals have found pronounced anisotropy of scale lengths of heterogeneity exhibited in textures closely related to directions of fluid flow above the solidifying solid boundary. These observations, coupled with the very different effects of anisotropically distributed scale lengths predicted on forward- versus back-scattered elastic wavefields, suggest that observations of PKiKP and PKiKP transmitted through and reflected by the same region of the inner core can be used to constrain the directions in which heterogeneity scale lengths are lengthened, the resultant anisotropy in velocity and attenuation, and the direction of fluid flow in the outer core above the inner core boundary.

Combining waveform and travel time observations, a qualitative model for the texture of the uppermost inner core has been proposed. Lateral variations in flow near the inner core boundary may be recorded in its texture. In this model the texture of the equatorial eastern hemisphere is characterized by either an isotropic distribution of heterogeneity scale lengths or an anisotropic distribution such that scale lengths are stretched vertically, perpendicular to the inner core boundary. It is suggested that this region of the inner core is currently the most rapidly solidifying, with an immediate overlying outer core enriched in lighter elements. This region is a source of relatively stronger upwelling in the liquid outer core, having relatively lower viscosity compared to adjacent regions, possibly accounting for greater turbulence and higher magnetic secular variation in the eastern hemisphere. The texture of the equatorial western hemisphere is more variable, but characterized by elongated length scales parallel to the inner core boundary. These elongations may be due to a process of isostatically induced flow and recrystallization that moves material from more actively crystallizing regions to less actively crystallizing regions [11]. The overlying outer core liquid in the

equatorial western hemisphere may be denser and have lower viscosity based on travel time models of this region. It may be characterized by localized downwellings that induce horizontally flattened-plate-like textures that strongly back scatter energy into the coda of PKiKP. Further testing of these textural variations should include: (1) a quantitative estimate of the relative importance of scattering versus viscoelasticity in the upper most inner core and its depth dependence, (2) observations of the back-scattered coda of PKiKP and the pulse broadening of transmitted PKiKP sampling identical regions of the inner core, (3) estimates and images of lateral heterogeneity in density and viscosity in the earth's outer core, and (4) geodynamo modeling to predict possible flow at the inner core boundary to estimate the relative importance of externally driven versus convectively driven flow near the inner core boundary.

## Acknowledgements

I thank Michael Bergman, Keith Koper, Amit Hagay, and Julien Aubert for their helpful comments and discussions. National Science Foundation Grant EAR 02-29586 supported this work.

## References

- [1] V.F. Cormier, L. Xu, G.L. Choy, Seismic attenuation of the inner core: viscoelastic or stratigraphic? *Geophys. Res. Lett.* 25 (1998) 4019–4025.
- [2] V.F. Cormier, X. Li, Frequency dependent attenuation in the inner core: Part II. A scattering and fabric interpretation, *J. Geophys. Res.* 107 (B12) (2002), doi:10.1029/2002JB1796.
- [3] J.E. Vidale, P.S. Earle, Fine-scale heterogeneity in the Earth's inner core, *Nature* 404 (2000) 273–275.
- [4] F. Leyton, K.D. Koper, Using PKiKP coda to determine inner core structure. 2. Determination of  $Q_c$ , *J. Geophys. Res.* (in press), doi:10.1029/2006JB004370.
- [5] D. Gubbins, T.G. Masters, J.A. Jacobs, Thermal evolution of the Earth's core, *Geophys. J. R. Astron. Soc.* 59 (1979) 57–99.
- [6] D. Gubbins, D. Alfè, G. Masters, G.D. Price, M. Gillan, Gross thermodynamics of two-component core convection, *Geophys. J. Int.* 157 (2004) 1407–1414.
- [7] M.I. Bergman, M. Macleod-Silberstein, M. Haskel, B. Chandler, N. Akpan, A laboratory model for solidification of Earth's core, *Phys. Earth Planet. Inter.* 153 (2005) 150–164.
- [8] M.I. Bergman, D.M. Cole, J.R. Jones, Preferred crystal orientations due to melt convection during directional solidification, *J. Geophys. Res.* 107 (B9) (2002), doi:10.1029/2001JB000601.
- [9] M.I. Bergman, S. Agrawal, M. Carter, M. Macleod-Silberstein, Transverse solidification textures in hexagonal closest packed alloys, *J. Cryst. Growth* 255 (2003) 204–211.
- [10] T.-K. Hong, R.-S. Wu, Scattering of elastic waves in geometrically anisotropic random media and its implication to sounding of heterogeneity in the Earth's deep interior, *Geophys. J. Int.* 163 (1) (2005) 324–338.

- [11] S. Yoshida, I. Sumita, M. Kumazawa, Growth model of the inner core coupled with the outer core dynamics and the resulting elastic anisotropy, *J. Geophys. Res.* 101 (1996) 28,085–28,103.
- [12] V.F. Cormier,  $D''$  as a transition in the heterogeneity spectrum of the lowermost mantle, *J. Geophys. Res.* 105 (2000) 16,193–16,205.
- [13] T. Furumura, B.L.N. Kennett, M. Furumura, Seismic wavefield calculation for laterally heterogeneous whole earth models using the pseudospectral method, *Geophys. J. Int.* 135 (1998) 845–860.
- [14] A.M. Dziewonski, D.L. Anderson, Preliminary Reference Earth Model (PREM), *Phys. Earth Planet. Inter.* 25 (1981) 297–356.
- [15] A. Frankel, R. Clayton, Simulation of seismic scattering, *J. Geophys. Res.* 91 (1986) 6465–6489.
- [16] S.N. Ward, Long-period reflected and converted upper mantle phases, *Bull. Seismol. Soc. Am.* 68 (1978) 133–153.
- [17] B. Kaelin, L.R. Johnson, Dynamic composite elastic medium theory. Part II. Three-dimensional media, *J. Appl. Phys.* 84 (1998) 5458–5468.
- [18] A. Stroujkova, V.F. Cormier, Regional variations in the uppermost 100 km of the Earth's inner core, *J. Geophys. Res.* 109 (B10) (2004), doi:10.1029/2004JB002976.
- [19] X. Song, D.V. Helmberger, Seismic evidence for an inner core transition zone, *Science* 282 (1998) 924–927.
- [20] G. Poupinet, B.L.N. Kennett, On the observation of high frequency PKiKP and its coda in Australia, *Phys. Earth Planet. Inter.* 146 (2004) 497–511.
- [21] H. Kawakatsu, Sharp and seismically transparent inner core revealed by an entire network observation of near-vertical PKiKP, *Earth Planets Space* 58 (2006) 855–863.
- [22] W. Yu, L. Wen, Inner core attenuation anisotropy, *Earth Planet. Sci. Lett.* 245 (2006) 581–594.
- [23] K.C. Creager, Anisotropy of the inner core from differential travel times of the phases of PKP and PKiKP, *Nature* 356 (1992) 309–314.
- [24] K.C. Creager, Large scale variations in inner core anisotropy, *J. Geophys. Res.* 104 (1999) 23127–23139.
- [25] K.C. Creager, Inner core anisotropy and rotation, in: S. Karato, et al., (Eds.), *Earth's Deep Interior: Mineral Physics and Tomography from the Atomic to the Global Scale*, *Geophys. Monogr. Ser.*, vol. 117, AGU, Washington, D. C., 2000, pp. 89–114.
- [26] S.I. Oreshin, L.P. Vinnik, Heterogeneity and anisotropy of seismic attenuation in the inner core, *Geophys. Res. Lett.* 31 (2004), doi:10.1029/2003GL018591.
- [27] A. Ouzounis, K.C. Creager, Isotropy overlying anisotropy at the top of the Earth's inner core, *Geophys. Res. Lett.* 28 (2001) 4331–4334.
- [28] X. Song, D.V. Helmberger, Depth dependence of anisotropy of Earth's inner core, *J. Geophys. Res.* 100 (1995) 9805–9816.
- [29] A. Souriau, B. Romanowicz, Anisotropy in inner core attenuation: a new type of data to constrain the nature of the solid core, *Geophys. Res. Lett.* 23 (1996) 1–4.
- [30] A. Souriau, B. Romanowicz, Anisotropy in the inner core: relation between P-velocity and attenuation, *Phys. Earth Planet. Inter.* 101 (1997) 33–47.
- [31] S. Tanaka, H. Hamaguchi, Degree one heterogeneity and hemispherical variation of anisotropy in the inner core from PKP (BC) and PKP(DF) times, *J. Geophys. Res.* 102 (1997) 2925–2938.
- [32] L. Wen, F. Niu, Seismic velocity and attenuation structures in the top of the Earth's inner core, *J. Geophys. Res.* 107 (B11) (2002), doi:10.1029/2001JB000170.
- [33] R. Garcia, Constraints on upper inner core structure from waveform inversion of core phases, *Geophys. J. Int.* 150 (2002) 851–864.
- [34] W. Yu, L. Wen, F. Niu, Seismic velocity structure in the Earth's outer core, *J. Geophys. Res.* 110 (2005), B02302, doi:10.1029/2003JB002928.
- [35] M.I. Bergman, Measurements of electric anisotropy due to solidification texturing and the implications for the Earth's inner core, *Nature* 389 (1997) 60–63.
- [36] W.F. Weeks, A.J. Gow, Preferred crystal orientations in the fast ice along the margins of the Arctic Ocean, *J. Geophys. Res.* 83 (1978) 5105–5121.
- [37] G. Steinle-Neumann, L. Stixrude, R.E. Cohen, O. Gulseren, Elasticity of iron at the temperature of the Earth's inner core, *Nature* 413 (2001) 57–60.
- [38] C.M.S. Gannarelli, D. Alfè, M.J. Gillan, The particle-in-cell model for ab initio thermodynamics: implications for the elastic anisotropy of the Earth's inner core, *Phys. Earth Planet. Inter.* 139 (2003) 243–253.
- [39] S.I. Karato, Seismic anisotropy of the Earth's inner core resulting from flow induced by Maxwell stresses, *Nature* 402 (1999) 871–873.
- [40] D. Gubbins, S.J. Gibbons, Low pacific secular variations, in: J.E.T. Channel, D.V. Kent, W. Lowrie, J.G. Meert (Eds.), *Timescales of the Paleomagnetic Field*, *AGU Monograph, Geodynamics Series*, vol. 145, 2004.
- [41] Z. Zou, K. Koper, V. Cormier, Constraints on the velocity gradient at the base of the outer core and inner core Q from PKP<sub>BC</sub> diffracted waves, *Eos, Trans. - Am. Geophys. Union* 87 (52) (2006) (Fall Meet. Suppl. (Abstract)).
- [42] D.N. Krasnoshchekov, P.B. Kaazik, V.M. Ovtchinnikov, Seismological evidence for mosaic structure of the surface of the Earth's inner core, *Nature* 435 (2005) 483–487.
- [43] D.J. Stevenson, Limits on lateral density and velocity variations in the Earth's outer core, *Geophys. J. R. Astron. Soc.* 88 (1987) 311–319.
- [44] G. Soldati, L. Boschi, A. Piersanti, Outer core density heterogeneity and the discrepancy between PKP and PcP travel times, *Geophys. Res. Lett.* 30 (2003), doi:10.1029/2002GL0166477.
- [45] A. Piersanti, L. Boschi, A.M. Dziewonski, Estimating lateral structure in the Earth's outer core, *Geophys. Res. Lett.* 28 (2001) 1659–1662.
- [46] S.-N. Luo, S. Ni, D. Helmberger, Relationship of  $D''$  structure with the velocity variations near the inner-core boundary, *Geophys. Res. Lett.* 29 (11) (2002) 1527–1530.
- [47] I. Sumita, P. Olson, A laboratory model for convection in Earth's core driven by a thermally heterogeneous mantle, *Science* 286 (1999) 1547–1549.